

Soap-film dynamics and topological transitions under continuous deformation*

H. K. Moffatt, Raymond E. Goldstein, and Adriana I. Pesci

*Department of Applied Mathematics and Theoretical Physics, University of Cambridge,
Wilberforce Road, Cambridge CB3 0WA, United Kingdom*

(Received 28 July 2016; published 18 October 2016)

The response of a soap film to the continuous deformation of its wire boundary is considered, with particular attention to the topological transitions that can occur at critical stages of the deformation process. Two well-known examples that have been studied by both theory and experiment are the catenoid suspended between circular wires in parallel planes, and the Möbius-strip soap film spanning a wire that is twisted and folded back on itself. In this latter case, we have shown in previous publications that, when the wire is unfolded, the soap film undergoes a topological transition through a boundary singularity to a two-sided film, with a corresponding jump in the linking number between the axis of the wire and the Plateau boundary on its surface. Here, we review this particular aspect of the problem, and propose a simplified model experiment through which the slipping adjustment of a Plateau border on a solid surface may be investigated.

DOI: [10.1103/PhysRevFluids.1.060503](https://doi.org/10.1103/PhysRevFluids.1.060503)

I. INTRODUCTION

A soap film bounded by a closed wire loop (or by several such wires, which may be knotted and/or linked) has minimum area with respect to small perturbations. This is because, under static boundary conditions, the energy E of the film relaxes to a minimum compatible with the topology of the configuration. Since $E = \sigma A$, where σ is the surface tension of the film, the area A is therefore minimized; in this equilibrium state, the Laplace pressure difference across the surface must vanish, from which it follows that the mean curvature of the surface is everywhere zero.

If the wire boundary is slowly and continuously deformed, such a surface generally evolves in a quasistatic manner, through a family of minimum-area states. However, at a certain stage it may become unstable, and it then jumps to a different topological configuration. Such a jump requires passage through a singularity. We have argued in a series of papers [1–4] that the collapse to a singularity is closely associated with a “systole” on the surface, i.e., a closed curve of locally minimum length that cannot be contracted on the surface to a point (in simple terms, it “goes round a hole in the surface”). If the systole is not linked with the boundary wire, then the singularity occurs at an interior point of the surface; if it is so linked, then the singularity necessarily occurs on the boundary.

The prototype in the former case is the classical catenoidal soap film bounded by two circular wires in parallel planes with a common axis; when these wires are slowly drawn apart, the minimum-area catenoid becomes unstable at a critical separation, and collapses on the axis.

In the second case, the prototype is the nonorientable Möbius strip; in this case, the systole encloses the hole through the strip and is linked with the wire boundary; the collapse is therefore to a point on the boundary [the bright spot in Fig. 1(a)]. We have shown [1] that, in order to understand the nature of the boundary singularity, it is necessary to take account of the finite radius of the wire. It is on this aspect of the problem that we focus in the present paper.

There are some obvious similarities with the problem of reconnection of magnetic flux tubes in a highly conducting fluid. Our study of soap-film dynamics has in part been motivated by the

*This paper is based on an invited lecture given by Keith Moffatt at the 68th Annual Meeting of the APS Division of Fluid Dynamics, which was held 22–24 November 2015 in Boston (MA), USA.

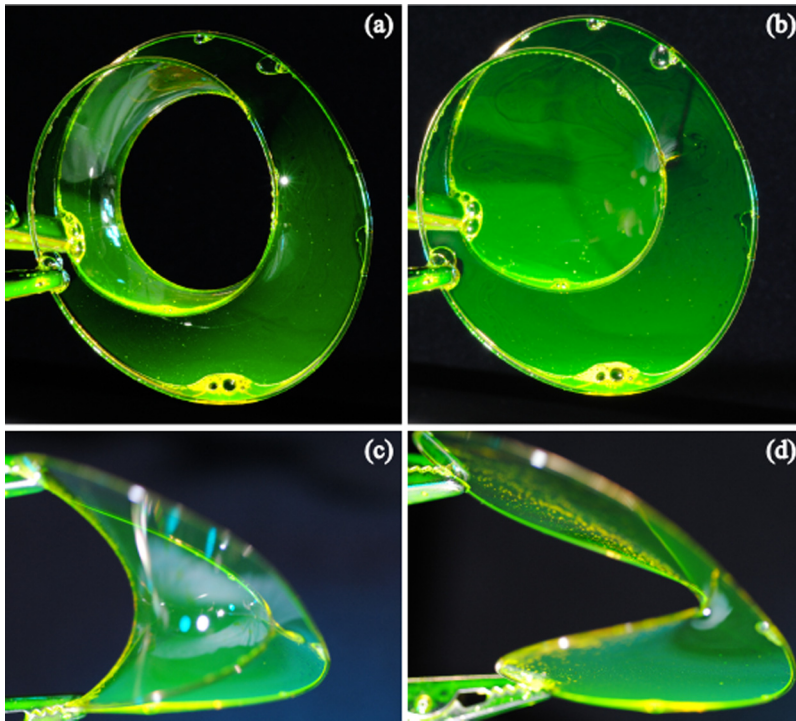


FIG. 1. Topological transition of a Möbius strip soap film, observed experimentally. Top (a) and side (c) views of a one-sided surface before the transition, and corresponding views [(b) and (d)] of the two-sided surface after the transition. Adapted from [1].

need to understand topological transitions in such (more complex) situations. The analogy with magnetic flux tubes is most evident in the context of the solar corona; here, the lines of force of the coronal field are anchored at “footpoints” on the solar photosphere, and the field evolves through minimum-energy states in response to movement of these footpoints caused by subsurface convective turbulence (for a recent review, see [5]). Under such forced evolution, the coronal field can collapse to a singular force-free state with imbedded tangential discontinuities (i.e., current sheets), in which Joule dissipation is largely responsible for the intense heating of the corona. For this scenario, we have the following correspondences:

magnetic field anchored on the photosphere	\iff	soap film with wire boundary,
movement of the footpoints	\iff	distortion of the wire boundary,
minimum magnetic energy	\iff	minimum surface area,
zero Lorentz force	\iff	zero mean curvature,
dissipative current sheets	\iff	viscous dissipation on the wire,
reconnection of field lines	\iff	topological transition of soap film.

The analogy is by no means perfect, but is at least suggestive. The great advantage of the soap-film model is that such topological transitions can be subjected to close experimental, as well as theoretical and computational, investigation.

SOAP-FILM DYNAMICS AND TOPOLOGICAL ...

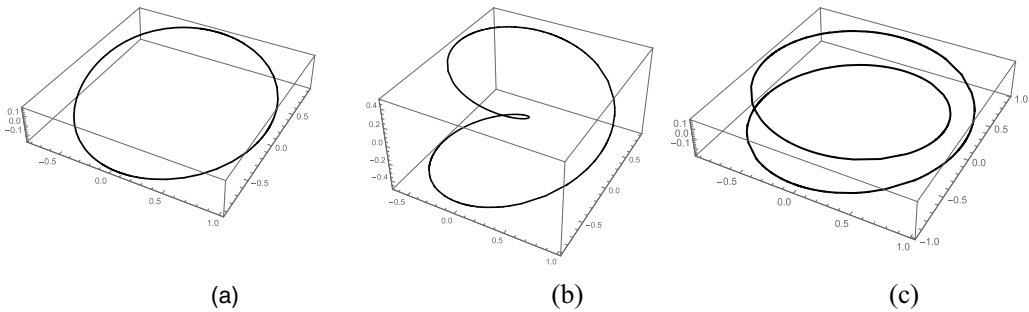


FIG. 2. Stretch-twist-fold, as represented by the evolving curve C parametrized by Eq. (1). (a) $t = 0.9$, (b) $t = 0.4$, and (c) $t = 0.1$.

II. STRETCH-TWIST-FOLD PROCESS

Further motivation comes from the “fast dynamo” mechanism conceived in Ref. [6] and treated in detail in Ref. [7]. This mechanism is one by which, in a perfectly conducting incompressible fluid, the intensity of a magnetic field may be doubled, and, by iteration on a constant time scale, increased exponentially; this provides a somewhat simplistic manifestation of “fast” dynamo action, so called because the growth rate is determined by the time scale of the flow, independent of magnetic diffusivity η in the limit $\eta \rightarrow 0$. Since we are dealing with quasistatic deformations, it suffices to describe parametrically a sequence of coordinate transformations with t denoting the (slow) time. The unfolding process may be parametrized [8] by the evolving curve $C : \mathbf{x}(s,t) = (x,y,z)$ with parametric equations

$$\begin{aligned} x(s,t) &= -t \cos s + (1-t) \cos 2s, \\ y(s,t) &= -t \sin s + (1-t) \sin 2s, \\ z(s,t) &= -2t(1-t) \sin s, \end{aligned} \quad (1)$$

where $-\pi < s \leq \pi$. As t increase from 0 to 1, the curve (1) “unfolds” from the double cover of a circle of unit radius in the x,y plane to the same circle described once (Fig. 2) [9].

The projection of the curve on the x,y plane shows a change of character as t passes through the value $2/3$; Fig. 3 shows this projection near $s = 0$ for $t = 0.65$, $2/3$, and 0.685 . At the instant $t = 2/3$, the projection has a cusp at $s = 0$, i.e., at the point $(-1/3, 0)$, and the three-dimensional curve C has locally the form of a twisted cubic with parametric equations, at leading order,

$$\mathbf{x}(s,t) \sim -\frac{1}{3} \left(1 + s^2, s^3, \frac{4}{3}s \right). \quad (2)$$

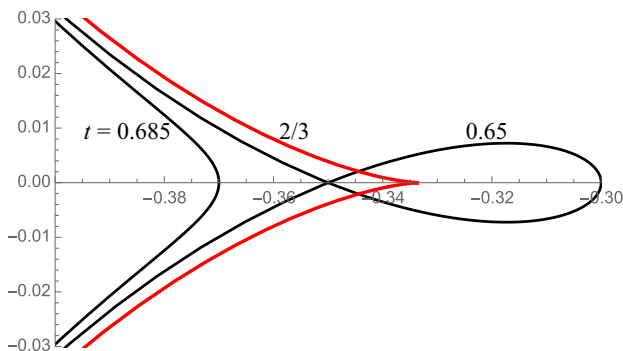


FIG. 3. Projection of the curve C on the x,y plane for $t = 0.65$, $2/3$, and 0.685 ; this projection has a cusp at $s = 0$ [i.e., at $(x,y) = (-1/3, 0)$], when $t = t_c = 2/3$, and the “hole” disappears as t increases through t_c .

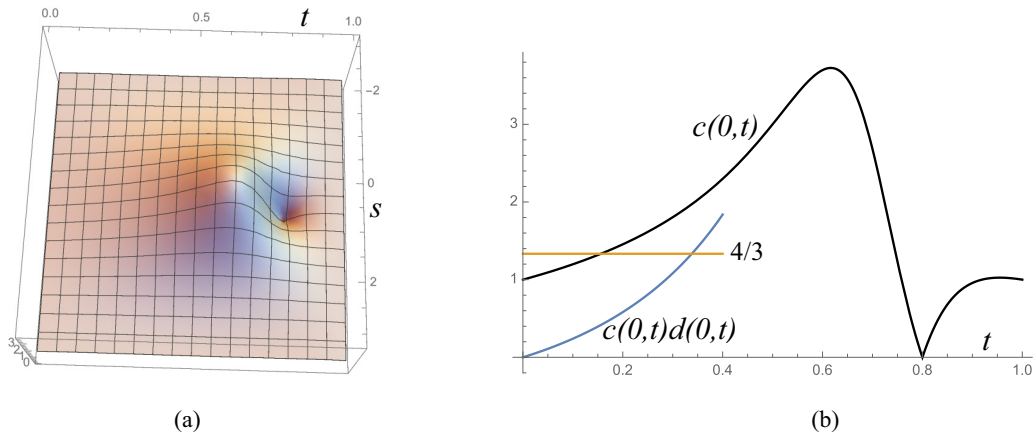


FIG. 4. (a) Plot of the curvature function $c(s,t)$, showing an isolated zero at $s = 0, t = 0.8$; (b) the function $c(0,t)$: as t passes through 0.8, the curve C passes through an inflexional configuration; also shown is the growth of $c(0,t)d(0,t)$ which reaches the level $4/3$ at $t \approx 0.338$.

For $t > 2/3$ the hole has disappeared, and the curve approaches a circle as t increases further towards 1.

The curvature $c(s,t)$ of C is given by

$$c(s,t) = |\mathbf{x}' \times \mathbf{x}''|/|\mathbf{x}'|^3, \quad (3)$$

where $(\prime) \equiv \partial/\partial s$. This function is shown in Fig. 4(a), and it is evident from Fig. 4(b) that $c(s,t) = 0$ at $s = 0, t = 4/5$; in fact, at $s = 0$, (3) reduces to

$$c(0,t) = \frac{|4 - 5t|}{4t^4 - 8t^3 + 13t^2 - 12t + 4}; \quad (4)$$

here, the quartic in the denominator is positive for all real t . The zero at $t = 4/5$ indicates an inflexion point at $s = 0$; the curve C may be said to “pass through an inflexional configuration” as t passes through $4/5$.

The separation of opposite points of the wire with parameters s and $s + \pi$ is given by the function $d(s,t) = |\mathbf{x}(s + \pi, t) - \mathbf{x}(s, t)|$. This separation is maximal at $s = 0$, and increases relative to the local radius of curvature c^{-1} as shown also in Fig. 4(b). The separation d reaches the level $\frac{4}{3}c^{-1}$ at $t \approx 0.34$; this is significant because it is the separation at which the catenoid collapses (see below).

It is interesting to compute the writhe $\text{Wr}(t)$ and twist $\text{Tw}(t)$ associated with this curve, which satisfy the well-known relationship $\text{Wr}(t) + \text{Tw}(t) = \text{const}$. The writhe depends only on the geometry of C , and is given by the Gauss integral

$$\text{Wr}(t) = \frac{1}{4\pi} \int_C \int_C \frac{(\mathbf{x} - \mathbf{x}') \cdot (\mathbf{dx} \times \mathbf{dx}')}{|\mathbf{x} - \mathbf{x}'|^3}. \quad (5)$$

The twist requires consideration of a ribbon with edges C and an adjacent curve C^* ; the twist (of the ribbon) is then given by

$$\text{Tw}(t) = \frac{1}{2\pi} \oint_C [\mathbf{N}'(s) \times \mathbf{N}(s)] \cdot d\mathbf{x}, \quad (6)$$

where $\mathbf{N}(s)$ is the unit normal to C on the ribbon, from C to C^* . One contribution to this twist involves the torsion $\tau(s,t)$ of the wire, given by the triple scalar product

$$\tau(s,t) = [\mathbf{x}', \mathbf{x}'', \mathbf{x}''']/|\mathbf{x}' \times \mathbf{x}''|^2. \quad (7)$$

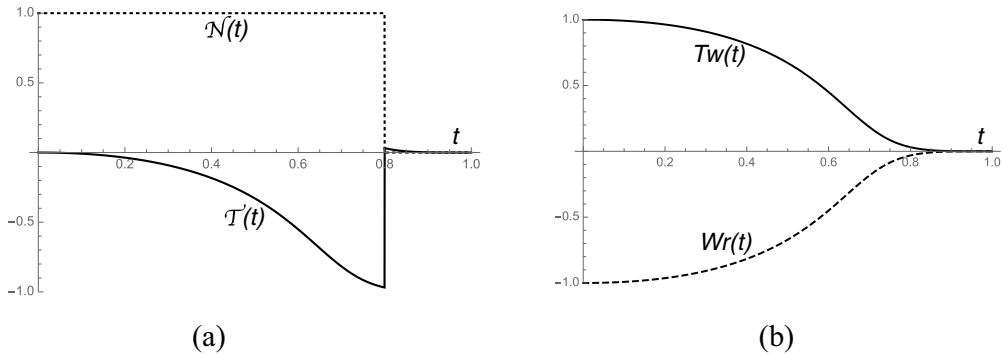


FIG. 5. (a) The integrated torsion $\mathcal{T}(t)$ (solid) showing the unit jump at $t = 4/5 = 0.8$ when C passes through an inflexional configuration, and the compensating “internal twist” $\mathcal{N}(t)$ (dotted); (b) the twist $\text{Tw}(t) = \mathcal{T} + \mathcal{N}$ (solid), and the writhe $\text{Wr}(t)$ (dashed) given by Eq. (5). Note that $\text{Wr}(t) + \text{Tw}(t) \equiv 0$.

If there are no inflexion points on C , and if the ribbon is twisted in such a way that $\mathbf{N}(s)$ makes a constant angle with the unit principal normal $\mathbf{n}(s)$ on C , then the twist is obtained by integrating this torsion round the curve:

$$\text{Tw}(t) = \mathcal{T}(t) = \frac{1}{2\pi} \oint_C \tau(s, t) |d\mathbf{x}/ds| ds. \quad (8)$$

More generally,

$$\text{Tw}(t) = \mathcal{T}(t) + \mathcal{N}, \quad (9)$$

where \mathcal{N} (an integer) is the number of turns of $\mathbf{N}(s)$ relative to the Frenet triad $\{\mathbf{t}, \mathbf{n}, \mathbf{b}\}$ in going around C . If C does have an inflexion point, then at this point $c = 0$ and τ is singular; as shown in [10], if C passes through an inflexional configuration, then $\mathcal{T}(t)$ is discontinuous by an amount ± 1 , with a compensating discontinuity ∓ 1 in \mathcal{N} .

For the curve C defined above, and with an untwisted ribbon at time $t = 1$, $\text{Wr}(1) = 0$ and $\text{Tw}(1) = 0$, and so $\text{Wr}(t) + \text{Tw}(t) \equiv 0$. Figure 5(a) shows the integrated torsion $\mathcal{T}(t)$ with the expected unit jump as t goes through $0.8 = 4/5$; and consequently $\mathcal{N} = 1$ for $0 < t < 4/5$, and $\mathcal{N} = 0$ for $4/5 < t < 1$. Figure 5(b) shows the twist $\text{Tw}(t)$ rising continuously from 0 to 1 as t decreases from 1 to 0, and the writhe $\text{Wr}(t)$ computed from (5), confirming that indeed $\text{Wr}(t) + \text{Tw}(t) \equiv 0$.

III. SOAP-FILM INSTABILITY

Recall first the situation when two equal circular wires $r = (x^2 + y^2)^{1/2} = a$ in planes $z = \pm b(t)$, bounding a catenoidal soap film, are gradually drawn apart. For any positive value of the ratio $\beta = b/a$, there is a one-parameter family of catenoids bounded by these circles, this family being described by the equation

$$r \cosh \lambda = a \cosh \lambda z/b \quad (0 \leq \lambda < \infty). \quad (10)$$

The area $A(\beta, \lambda)$ of these catenoids is easily calculated; this function is shown in Fig. 6. For $\beta < \beta_c \approx 0.6627$, just slightly less than $2/3$, the curve has two extrema, a minimum and a maximum which move to coincidence at an inflexion point as β increases to the critical value β_c . Thus a minimum-area catenoidal soap film exists for $\beta < \beta_c$, but becomes unstable at $\beta = \beta_c$, and for $\beta > \beta_c$ there is no smooth minimum-area solution of catenoidal form: for $\beta > \beta_c$, the film collapses to a viscous thread on the axis coupled with discs spanning each wire (the “Goldschmidt solution” [11]). Details of the collapse process and the subsequent breakup of the thread have been described in Refs. [12, 13].

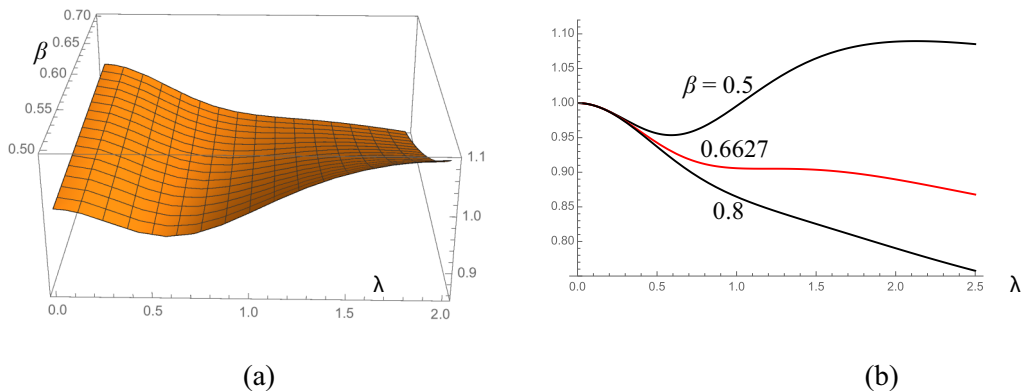


FIG. 6. (a) The area $A(\beta, \lambda)/4\pi ab$ of catenoids bounded by wires $r = a, z = \pm b$ (with $\beta = b/a$) for $0.5 < \beta < 0.7$, and $0 < \lambda < 2$; (b) the same area function for $\beta = 0.5, 0.6627, 0.8$; there is an inflexion point when $\beta = \beta_c \approx 0.6627$, at which stage the surface becomes unstable; for $\beta > \beta_c$, there is no minimum area solution.

Turning now to the one-sided Möbius strip, a soap film with this topology can be obtained by dipping a wire, shaped as in Fig. 2(c) at parameter value $t \approx 0.1$, in soap solution, and puncturing the two-sided disc that usually forms; a one-sided soap film with the topology of a Möbius strip then remains. If now the wire is slowly unfolded, then collapse occurs at a certain stage, actually around $t = 0.4$; as shown in Fig. 4, the product $d(0, t)c(0, t)$ exceeds the level $4/3$ by this stage, admitting comparison as indicated earlier with the catenoidal collapse. Here, the collapse indeed proceeds to an apparent singularity on the boundary wire, through which the one-sided Möbius strip jumps to a two-sided surface (topologically a disk) spanning the wire.

We can gain some understanding of this process through consideration of the ruled surface S_r with parametric equations

$$\begin{aligned} x(s, \mu, t) &= \mu t \cos s + (1 - t) \cos 2s, \\ y(s, \mu, t) &= \mu t \sin s + (1 - t) \sin 2s, \\ z(s, \mu, t) &= 2\mu t(1 - t) \sin s, \end{aligned} \tag{11}$$

for $-1 \leq \mu \leq 1, -\pi \leq s < \pi$, as shown in Fig. 7(a) for parameter value $t = 0.3$. This is not a minimal surface; it is rather a surface that can be formed by a rectangular strip of paper twisted

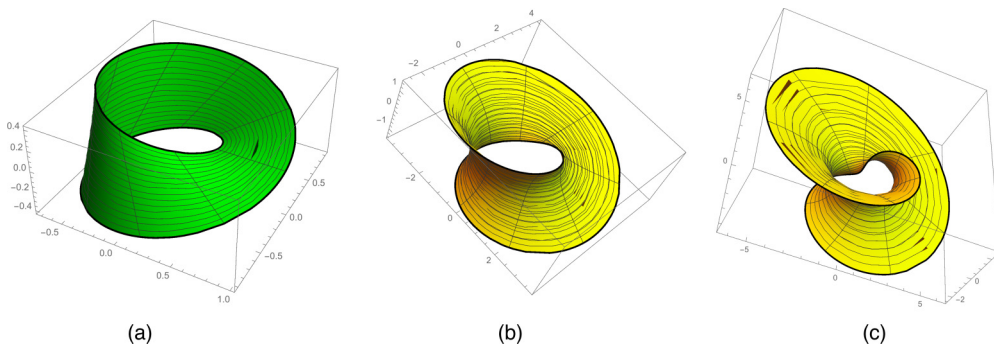


FIG. 7. (a) The ruled surface S_r described by (11) at parameter value $t = 0.3$. (b) The Meeks minimal surface S_M with parametric equations (12), at parameter value $r_0 = 0.7$. (c) The Meeks surface at parameter value $r_0 = 0.54$, when it becomes unstable.

through an angle π and with the ends joined to form a Möbius strip. Note that the section of this surface at $\mu = 0$ is a circle of radius $1 - t$ in the z plane.

A true minimal surface with the Möbius-strip topology, as found in Ref. [14], is given by the (incomplete) “Meeks minimal surface” S_M shown in Fig. 7(b), given in terms of functions $\alpha(r) = r - 1/r$, $\beta(r) = r^2 + 1/r^2$, $\gamma(r) = \frac{1}{3}(r^3 - 1/r^3)$ by parametric equations

$$\begin{aligned} x(r,s,t) &= -\alpha \sin s - \beta \sin 2s - \gamma \sin 3s, \\ y(r,s,t) &= \alpha \cos s + \beta \cos 2s + \gamma \cos 3s, \\ z(r,s,t) &= 2\alpha \sin s, \end{aligned} \tag{12}$$

for $-\pi \leq s < \pi$, $r_0 \leq r \leq 1/r_0$. The boundary curves in Figs. 7(a) and 7(b) are quite similar, but the surfaces, although topologically equivalent, are geometrically quite different, in that the Meeks surface contracts inwards in such a way as to achieve zero mean curvature at each point. This inward contraction, resembling the contraction of the catenoid, is most marked where the normal separation of the two strands of the wire is greatest, and it is in this neighborhood that the collapse process is initiated with gradually increasing separation.

We note that the boundary curve $r = r_0$ of S_M evolves as r_0 decreases from 1 to 0 from the double cover of a circle of radius 2 at $r_0 = 1$ to a *triple* cover of a “circle at infinity” at $r_0 = 0$. However, in the range $1 > r_0 \gtrsim 0.7$, the evolution replicates quite well the early stage of the unfold-untwist process; the parameter value $r_0 = 0.7$ is chosen by way of illustration in Fig. 7(b). As shown in Ref. [4], with further decrease of r_0 , the Meeks surface becomes unstable at the critical value $r_0 \approx 0.54$ [Fig. 7(c)]; the influence of the γ terms in Eq. (12) is already evident at this stage.

IV. INTERACTION OF SOAP FILM WITH WIRE SURFACE

It was already evident in our initial experiment [1] that account must be taken of the finite wire radius, and of the Plateau boundary on the wire, in order to understand the nature of the collapse singularity. The Plateau boundary is the curve where the continuation of the soap film intersects the surface of the supporting wire; accumulation of fluid in the immediate neighborhood of this curve allows visualization of the Plateau boundary in experiments. The wire itself was twisted in a left-handed sense (positive writhe), and we observed that just before the singularity, the Plateau boundary was locally twisted around the wire in a left-handed sense, and just after the singularity in a right-handed sense. (If the wire is instead twisted in a right-handed sense, then all handedness is reversed.) Figures 8(a) and 8(b) shows at least qualitatively (and that, after all, is what matters here) the situation before and after the transition; the radius of the wire is deliberately expanded to make the situation more visible. The configuration of the Plateau boundary before and after the transition is shown (in green) in Figs. 8(c) and 8(d); before the transition, it is doubly linked with the wire center line (shown in black), the successive crossings being “under, over, under, over.” The first “under, over” pair here corresponds to the left-handed twist near the collapse region (where $|s|$ is small); the switch to a right-handed twist replaces this pair by “over, under” producing in total “over, under, under, over.” The “under, under” pair can now be removed by sliding this portion of the green curve across the black curve; then similarly the remaining “over, over” pair can be removed. The net effect of the switch is therefore to replace the double linkage by a zero linkage, as shown in Fig. 8(d), where the green and black curves are obviously unlinked.

There remains the problem of understanding exactly what happens when the soap film impacts the wire boundary at the moment of collapse. This is difficult because of the three-dimensionality of the interaction associated with the peculiar Möbius-strip geometry. In order to isolate some salient features of the interaction between the soap film and the solid wire boundary, we propose the following model problem, as illustrated schematically in Fig. 9.

Imagine a catenoidal soap film suspended between two circular wires of radius a , drawn apart to separation $2b = 4a/3$, i.e., just above the critical separation at which collapse first occurs. Imagine

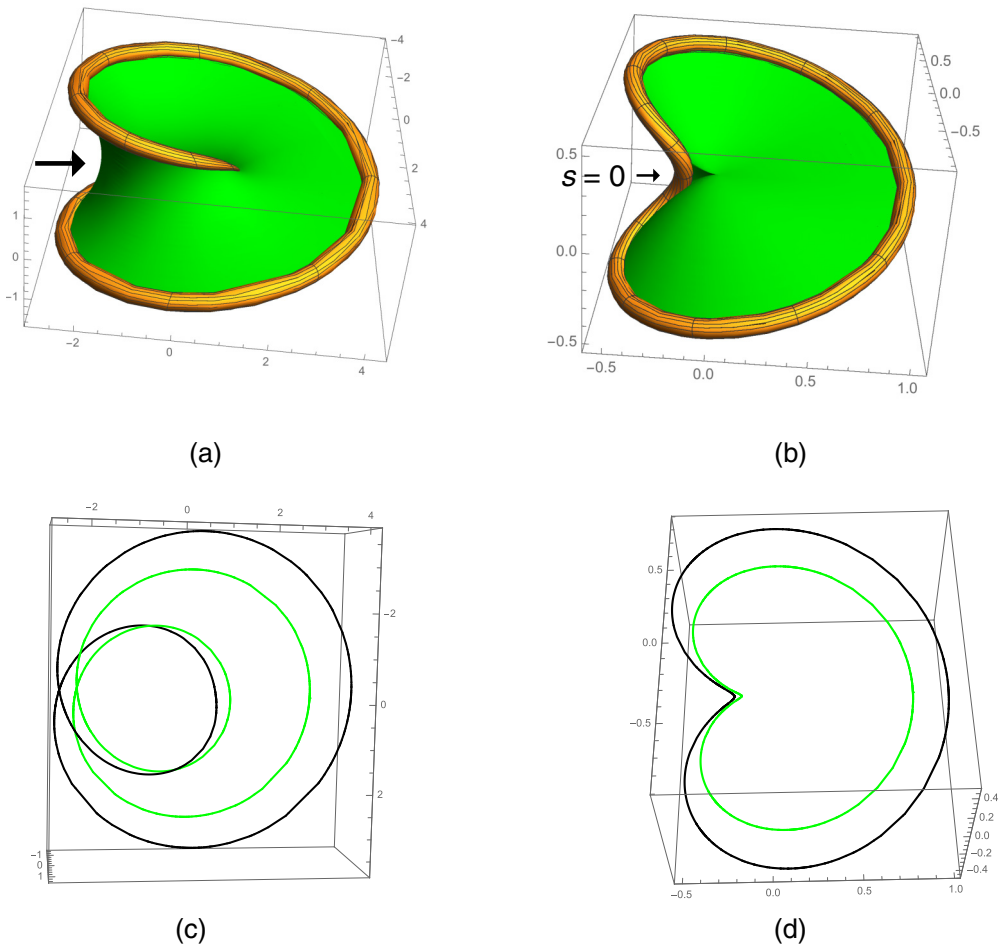


FIG. 8. (a) The one-sided Meeks minimal surface at parameter value $r_0 = 0.7$, as in Fig. 7(b); collapse is initiated in the direction of the arrow where the opposite strands of the wire are most separated. (b) A two-sided surface of disk topology spanning the wire C of Eq. (1) at $t = 0.6$, well before its passage through the inflexional configuration at $t = 0.8$; at this stage, $\text{Tw}(t) \approx 0.45$ and the surface is strongly distorted near $s = 0$, as observed in the experiment of [1] (cf. Fig. 2). (c) Plateau boundary (green) corresponding to (a), showing double linkage “under, over, under, over” with the wire center line (black) before the jump. (d) Plateau boundary corresponding to (b), now unlinked with the wire.

further that a cylindrical rod of radius δ ($< a$) is placed symmetrically on the axis. The catenoid must collapse and impact the rod on a circular line of contact [Fig. 9(a)]; from this point on, the soap-film area can decrease further by continuous contraction of the two “half films,” with limiting state two annular discs between the wires and the rod [Fig. 9(b)]—cf. the Goldschmidt solution]. Our interest focuses on the associated migration of the two Plateau boundaries along the rod.

Considering just the upper soap film, suppose that the Plateau border is at $z = Z(t)$ at time t [with $0 < Z(t) < b$], where we now measure t from the moment of impact. The area of the film is a decreasing function of Z : $A = A[Z(t)]$ [with $A'(Z) < 0$], and its surface-tension energy is $E = \sigma A$; hence

$$dE/dt = \sigma A'(Z)dZ/dt. \quad (13)$$

SOAP-FILM DYNAMICS AND TOPOLOGICAL ...

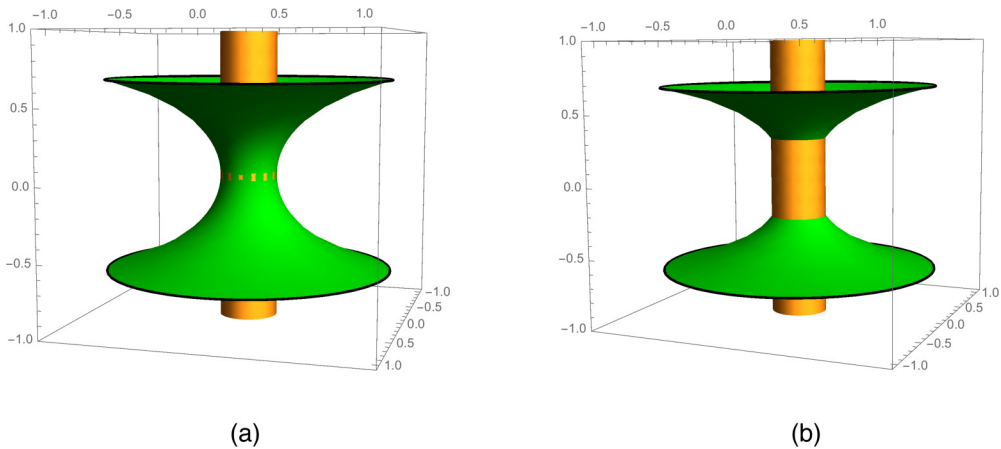


FIG. 9. (a) Collapsing catenoidal soap film at the instant at which it impacts a rod on the axis of symmetry; (b) subsequent collapse to two annular rings, with migration of Plateau boundaries along the rod.

Assuming for simplicity that $\delta \ll a$, we have $A(b) \approx \pi a^2$ and $A(0) \sim 1.2A(b)$ and so, in order of magnitude (with $b = \frac{2}{3}a$), $A'(Z) \sim -0.2\pi a^2/b \sim -0.3\pi a$. Hence

$$-dE/dt \sim 0.3\pi\sigma aU(t), \quad (14)$$

where $U(t) = dZ/dt$, the speed of migration of the Plateau boundary.

The rate of decrease of energy (14) must presumably be accommodated by the total rate of viscous dissipation of energy Φ due to the slipping of the Plateau boundary along the wire, assuming that this is the dominant dissipative mechanism. Suppose that the rod is prewetted, and that the film thickness on the rod is $h(\ll\delta)$. Then the strain rate in the neighborhood of the Plateau boundary is of order U/h ; this extends over a volume of order $(2\pi\delta)h^2$ and so, again in order of magnitude, $\Phi \sim \mu(U/h)^2(2\pi\delta)h^2 \sim 2\pi\mu U^2\delta$. Hence

$$0.3\pi\sigma aU \sim 2\pi\mu U^2\delta, \quad (15)$$

and so, in order of magnitude,

$$U \sim 0.15(\sigma/\mu)(a/\delta). \quad (16)$$

A second (equivalent) method of obtaining this estimate involves consideration of the forces acting on the soap film when it is in contact with the rod. Surface tension at the wire exerts on the film a net upward force with vertical component $F_{z1} = 2\pi a\sigma \cos \alpha$, where α is the angle between the tangent to the film in any meridian plane and the vertical. Neglecting inertia, this force must be compensated by a *downward* force F_{z2} , due to viscous drag exerted over the vertical scale h of the Plateau boundary on the rod. The viscous stress τ in this region is of order $\tau \sim \mu U/h$ and this is exerted over an area of order $2\pi\delta h$; hence $F_{z2} \sim 2\pi\mu\delta U$. The force balance $F_{z1} = F_{z2}$ then gives

$$U \sim \langle \cos \alpha \rangle (\sigma/\mu)(a/\delta), \quad (17)$$

where $\langle \cos \alpha \rangle$ is an appropriate mean value. This estimate may be compared with (16). We note that, for the configuration of Fig. 9, α increases from about $2\pi/5$ ($\cos \alpha \approx 0.28$) to $\pi/2$ ($\cos \alpha = 0$) as the migration proceeds, so a mean value $\langle \cos \alpha \rangle \approx 0.15$ is not unreasonable; in other words, the estimates (16) and (17) are entirely compatible.

These are admittedly crude arguments, and have obvious limitations, but they nevertheless provide a preliminary order-of-magnitude estimate that can be subjected to experimental test. For a soap solution with viscosity about five times that of water, σ/μ is of order 1 m/s, so that with a/δ about

MOFFATT, GOLDSTEIN, AND PESCI

5 say, the velocity U will be of order 75 cm/s. If $a \sim 3$ cm, the Plateau border should, for such a system, relax to an annular disc in a time of order 10^{-2} s.

Details of this experiment, currently under development, will be provided in a future publication.

V. DISCUSSION

Soap-film dynamics offers a wealth of fascinating problems, which invite theoretical and experimental investigation. First, there is the link with the great mathematical field of minimal surfaces initiated by the early work of Euler on the catenoid. A huge literature exists on this subject, but relatively little on the *dynamics* of soap films under continuous boundary deformation, and particularly on the topological transitions that such deformation can provoke. As we have shown in earlier publications, such transitions can occur through singularities at the soap-film boundary, and the nature of the transitions can be understood by taking account of the finite radius of the boundary wire. We are then faced with the problem of a minimal area surface bounded not by a prescribed curve C , but rather by the surface S_w of the wire on which the Plateau boundary is free to move in response to surface-tension forces, such motion being resisted by viscosity in the immediate neighborhood of the wire surface.

The transition of the catenoid to the Goldschmidt solution involves a singularity in the interior of the film, rather than on its boundary, and resolution of the singularity in a real fluid involves breakup of a viscous thread into droplets on the axis of symmetry; here, surface tension, viscosity, and inertia all play a part in the breakup process. Singularity problems of this kind are well described in the recent book of Eggers and Fontalo [15].

There is also a wealth of problems involving the internal dynamics of soap films, both as regards oscillations of the films in stable regimes, and as regards vortical flow within the film generated again by viscous effects at the film boundary.

Singularity problems arise in many related fields of fluid mechanics, in particular problems of key importance concerning vortex reconnection at high Reynolds number, or magnetic-flux tube reconnection in high conductivity magnetohydrodynamics; these problems involve near singular situations which are similarly resolved by viscous or finite conductivity effects at the moment of topological transition. Soap-film transitions are similar in some respects, and easier to investigate both theoretically and experimentally—a powerful motivation for continuing studies in this field!

ACKNOWLEDGMENTS

Discussions with A. Goriely on the subject of this paper are gratefully acknowledged. This work was supported in part by EPSRC Established Career Fellowship No. EP/M017982/1 (R.E.G. and A.I.P.).

-
- [1] R. E. Goldstein, H. K. Moffatt, A. I. Pesci, and R. L. Ricca, Soap-film Möbius strip changes topology with a twist singularity, *Proc. Natl. Acad. Sci. USA* **107**, 21979 (2010).
 - [2] R. E. Goldstein, H. K. Moffatt, and A. I. Pesci, Topological constraints and their breakdown in dynamical evolution, *Nonlinearity* **25**, R85 (2012).
 - [3] R. E. Goldstein, J. McTavish, H. K. Moffatt, and A. I. Pesci, Boundary singularities produced by the motion of soap films, *Proc. Natl. Acad. Sci. USA* **111**, 8339 (2014).
 - [4] A. I. Pesci, R. Goldstein, G. Alexander, and H. K. Moffatt, Instability of a Möbius Strip Minimal Surface and a Link with Systolic Geometry, *Phys. Rev. Lett.* **114**, 127801 (2015).
 - [5] S. Inoue, Magnetohydrodynamics modeling of coronal magnetic field and solar eruptions based on the photospheric magnetic field, *Prog. Earth Planet. Sci.* **3**, 19 (2016).

SOAP-FILM DYNAMICS AND TOPOLOGICAL ...

- [6] S. I. Vainshtein and Y. B. Zel'dovich, Origin of magnetic fields in astrophysics, *Sov. Phys. Usp.* **15**, 159 (1972).
- [7] S. Childress and A. D. Gilbert, *Stretch, Twist, Fold: The Fast Dynamo*, Lecture Notes in Physics No. 406 (Springer, New York, 1995).
- [8] F. Maggioni and R. L. Ricca, Writhing and coiling of closed filaments, *Proc. R. Soc. A* **462**, 3151 (2006).
- [9] The stretch-twist-fold sequence occurs for *decreasing* t ; the inverse process for increasing t , which is more convenient for the discussion of the present paper, is better described by the sequence unfold-untwist-relax.
- [10] H. K. Moffatt and R. L. Ricca, Helicity and the Călugăreanu invariant, *Proc. R. Soc. A* **439**, 411 (1992).
- [11] B. Goldschmidt, *Determinatio Superficie Minimae Rotatione Curvae Data Duo Puncta Jungentis circa Datum Axem Ortae*, Phil. Preisschr. Vol. 4 (Gottingae Dieterich, Göttingen, 1831).
- [12] N. D. Robinson and P. H. Steen, Observations of singularity formation during the capillary collapse and bubble pinch-off of a soap film bridge, *J. Colloid Interface Sci.* **241**, 448 (2001).
- [13] M. Nitsche and P. H. Steen, Numerical simulations of inviscid capillary pinchoff, *J. Comput. Phys.* **200**, 299 (2004).
- [14] W. H. I. Meeks, The classification of complete minimal surfaces in R^3 with total curvature greater than -8π , *Duke Math. J.* **48**, 523 (1981).
- [15] J. Eggers and M. A. Fontelos, *Singularities: Formation, Structure, and Propagation*, Cambridge Texts in Applied Mathematics, Vol. 53 (Cambridge University Press, Cambridge, England, 2015).